J. Fluid Mech. (1982), *vol.* 123, *pp.* 363–378
Printed in Great Britain

The effects of surface roughness on the flow past circular cylinders at high Reynolds numbers

By Y. NAKAMURA AND Y. TOMONARI†
Research Institute for Applied Mechanics, Kyushu University, Fukuoka, Japan

(Received 17 June 1981)

Measurements of the mean-pressure distribution and the Strouhal number on a smooth circular cylinder, circular cylinders with distributed roughness, and circular cylinders with narrow roughness strips were made over a Reynolds-number range $4{\cdot}0 \times 10^4$ to $1{\cdot}7 \times 10^6$ in a uniform flow. A successful high-Reynolds-number (trans-critical) simulation for a smooth circular cylinder is obtained using a smooth circular cylinder with roughness strips. High-Reynolds-number simulation can only be obtained by roughness strips and not by distributed roughness. A similarity parameter correlating the pressure distributions on circular cylinders with distributed roughness in the supercritical range is presented. The same parameter can also be applicable to the drag coefficients of spheres with distributed roughness.

1. Introduction

The flow past circular cylinders at high Reynolds numbers has long been a subject of intense attention both from academic and practical points of view. The subject is concerned with the complicated interaction between the transition and separation of boundary layer on rounded surface, while it is related to huge engineering structures such as tall stacks, cooling towers and offshore platforms. A number of papers have been written on this subject. These include Fage & Warsap (1929), Roshko (1961), Tani (1964, 1967), Jones, Cincotta & Walker (1969), Achenbach (1968, 1971, 1977), Szechenyi (1975), Güven, Patel & Farell (1977), Güven, Farell & Patel (1980) and Farell (1981). In particular, an extensive comparison of previous experimental data is found in Güven *et al.* (1980).

It has now been well recognized that surface roughness can not only promote the boundary-layer transition from laminar to turbulent, but also affect significantly the subsequent flow development at Reynolds numbers well beyond the critical. This was noticed as early as in 1929 by Fage & Warsap (1929), but recent experimental investigations (Roshko 1970; Szechenyi 1975) have suggested that even small roughness of an order of rD of 10^{-5} to 10^{-4}, where r and D are the size of roughness and the cylinder diameter respectively, may be influential on the flow past a seemingly smooth circular cylinder at high Reynolds numbers. On the other hand, Güven *et al.* (1977) proposed an analytical model theory, based on the Stratford–Townsend theory for turbulent separation combined with the wake–source model of Parkinson and Jandali, for the flow past a circular cylinder with distributed roughness at Reynolds numbers well beyond the critical.

Despite these efforts, information that has been obtained on this subject still remains far from complete. It is thus necessary to make further investigations, either

† Present address: Department of Aeronautical Engineering, Ohita Institute of Technology, Ohita, Japan.

experimental or analytical, to understand the precise role played by roughness on the flow past circular cylinders at high Reynolds numbers.

It is often difficult to realize in conventional wind tunnels the high-Reynolds-number flow past a smooth circular cylinder. Artificial transition of a boundary layer due to roughness may provide a means of producing the effective high-Reynolds-number flow at relatively low Reynolds numbers. Based on this idea, Tani (1964) proposed a method of using tripping wires, and with this method he succeeded in obtaining the transcritical flow (see figure 1) past an otherwise smooth circular cylinder at a Reynolds number of $4{\cdot}7 \times 10^5$. The technique of high-Reynolds-number simulation cannot avoid the problem of the effect of surface roughness, since, as mentioned above, even very small roughness may be influential. In other words, an exploration of any successful technique of simulation can provide an opportunity to investigate the significant effect of surface roughness on the flow past circular cylinders at high Reynolds numbers.

This paper presents the results of an experimental investigation undertaken to elucidate the vital effect of surface roughness on the mean-pressure distribution and the Strouhal number. Cylinders with various types of surface roughness were examined over the Reynolds number range $4{\cdot}0 \times 10^4$–$1{\cdot}7 \times 10^6$ in a uniform flow. These include a smooth cylinder, cylinders with distributed roughness and cylinders with narrow roughness strips. In §§2–4 experimental arrangements, measurement procedures, and the terminology and comparison with other works are given. The results of measurement are described in §5, where the effects of distributed roughness on the mean-pressure distribution and the Strouhal number, and the high-Reynolds-number simulation using a smooth circular cylinder with roughness strips, are discussed in detail, together with the presentation of a similarity parameter correlating circular cylinders and spheres with distributed roughness at high Reynolds numbers. Finally, conclusions are given in §6.

2. Experimental arrangements

2.1. *Wind tunnel and models*

The experiments were conducted in a low-speed wind tunnel with a 4 m high by 2 m wide by 6 m long rectangular working section. The flow in the working section was reasonably uniform with a turbulent intensity of about 0·12%. A point where the reference static and total pressures could be measured was chosen on the basis of the longitudinal traverses ahead of the model.

A 0·62 m diameter PVC circular-cylinder model was mounted horizontally in the working section with its axis on the tunnel centreplane 2·0 m downstream of the end of the tunnel contraction. The length-to-diameter ratio of the cylinder l/D was therefore equal to 3·33, while the blockage ratio, defined as the cylinder diameter divided by the working-section height D/H, was equal to 0·155. Thirty-six pressure taps were drilled at every 10° along a meridian of the cylinder at its midspan, and eight additional pressure taps were provided along a generator at the base of the cylinder.

2.2. *Surface roughnesses*

The major types of surface roughness examined in this study are listed in table 1. In the experiments on a smooth cylinder, the cylinder surface was polished as smooth as possible, although the degree of smoothness could not be specified quantitatively. In the experiments on cylinders with distributed roughness, polystyrene particles of

Condition of roughness	Size r of roughness particles	r/D
Smooth	—	—
Distributed roughness over whole surface	6·2 mm	1000×10^{-5}
Distributed roughness over whole surface	3·2 mm	516×10^{-5}
Distributed roughness over whole surface	1·4 mm	226×10^{-5}
Distributed roughness over whole surface	0·56 mm	90×10^{-5}
Distributed roughness over $\theta = 50°$–$130°$	3·2 mm	516×10^{-5}
Smooth with 3·2 mm diameter roughness strips of width 2 cm at $\theta = 50°$		
Distributed roughness over $\theta = 50° - 180°$ with roughness strips as above	0·56 mm	90×10^{-5}
Distributed roughness over $\theta = 50°$–$180°$ with roughness strips as above	115 μm (sandpaper, C-100)	$18{\cdot}5 \times 10^{-5}$
Distributed roughness over $\theta = 50°$–$180°$ with roughness strips as above	58 μm (sandpaper, C-180)	$9{\cdot}4 \times 10^{-5}$
Distributed roughness over $\theta = 50°$–$180°$ with roughness strips as above	40 μm (sandpaper, C-400)	$6{\cdot}5 \times 10^{-5}$

TABLE 1. Major types of surface roughness examined in this study

approximately the same size were glued as roughness elements onto the cylinder surface by using two-sided adhesive tape. The four different sizes of particles examined were 6·2, 3·2, 1·4 and 0·56 mm. Particles smaller than these were tried but it was found to be difficult to glue them in a single layer. In these experiments, particles were densely distributed over the whole cylinder surface except for the case of $r = 3{\cdot}2$ mm, where measurements were added on a cylinder with roughness that was distributed in a restricted range $\theta = 50°$–$130°$ on the upper and lower sides, θ being the meridional angle measured from the forward stagnation point.

In the experiments that followed, roughness strips of 2 cm in width consisting of a rather sparse distribution of 3·2 mm diameter polystyrene particles were glued to the upper and lower sides of a cylinder at $\theta = 50°$. The condition of the cylinder surface downstream of the roughness strips was varied from smooth to rough, as shown in table 1. The coarsest roughnesses used were 0·56 mm diameter polystyrene particles. For finer roughnesses, commercial sandpaper was wrapped around the cylinder in two pieces, with the seam located at the base of the cylinder. The sandpaper used had three different grain sizes. Although the grain sizes were not measured, the average values quoted by the manufacturer are listed in table 1. The manufacturer also quoted that the thickness of the adhesive material is approximately half the average grain size.

3. Measurement procedures

The range of Reynolds number R covered in the present study was $4{\cdot}0 \times 10^4$–$1{\cdot}7 \times 10^6$ approximately. Measurements of the mean static pressures were made by means of a calibrated inductance-type pressure transducer in conjunction with a 48-terminal scanivalve and an amplifier with a low-pass filter. The frequency of regular vortex shedding behind a cylinder was measured with a hot-wire set at a location $1{\cdot}5D$ downstream of the base of the cylinder and $1\,D$ down the tunnel centreline.

The results of measurement are presented in terms of the pressure coefficient C_p, the drag coefficient C_d and the Strouhal number S. Here C_p, C_d and S are defined

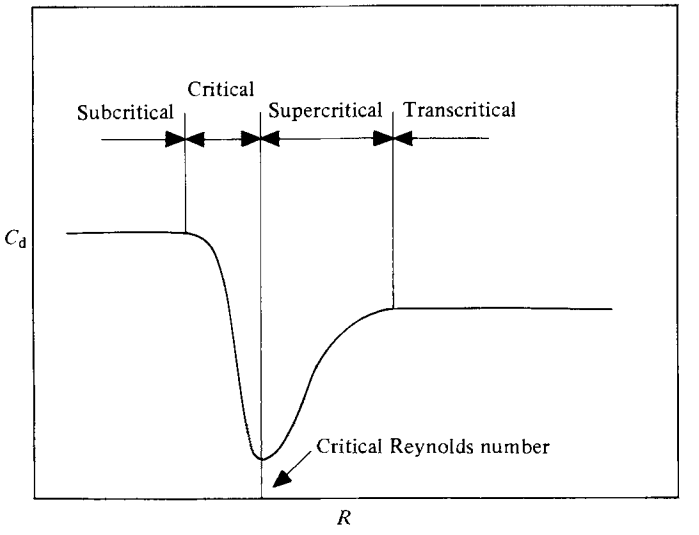

FIGURE 1. Four Reynolds-number ranges relevant to the flow past circular cylinders.

by $C_p = (p-p_0)/\frac{1}{2}\rho V^2$, $C_d = F/\frac{1}{2}\rho V^2 D$ and $S = f_v D/V$, where p is the mean static pressure on the cylinder surface, ρ, p_0 and V are respectively the air density, static pressure and speed of the uniform approaching flow, and f_v is the frequency of vortex shedding behind a cylinder. In particular, the results of measurement for the base pressure coefficient C_{pb} and the pressure recovery $C_{pb}-C_{pm}$, where C_{pm} is the minimum pressure coefficient, are also presented. The present data have been corrected for blockage according to the procedure of Allen & Vincenti (1944). The data shown in the subsequent figures are all corrected ones unless otherwise stated.

4. Terminology and comparison with other works

There are four different high-Reynolds-number flow ranges relevant to a circular cylinder. The terminology and the definitions themselves vary among authors. As is shown in the sketch of figure 1, the terminology and the definitions of the present paper are based on the drag coefficient versus Reynolds number curve. The four ranges are referred to as the subcritical, the critical, the supercritical and the transcritical ranges, with the critical Reynolds number being identified as that giving the minimum C_d.

Historically, Roshko (1961) was the first who proposed the classification of the flow ranges related to a smooth circular cylinder at high Reynolds numbers. He advocated the following terminology: at subcritical Reynolds numbers the separation is laminar; in the supercritical range there is a laminar separation bubble followed by turbulent separation; and in the transcritical range the separation is purely turbulent. Later, some people, including Achenbach (1977) and Farell (1981), modified Roshko's terminology by introducing a new term, the critical range. According to Farell (1981), each of these ranges is characterized by the special boundary-layer behaviour: subcritical (purely laminar separation); critical (laminar bubbles followed by turbulent reattachment and delayed final separation); supercritical (transition ahead of separation and moving upstream); and transcritical (transition sufficiently close to the stagnation point that the flow becomes independent of R). Thus, in the new

terminology, laminar bubbles vanish at the beginning of the supercritical range rather than at its end as Roshko guessed earlier. This terminology, which is based on the physics of the flow, has been used in most of the previous investigations.

Broadly speaking, the terminology based on the physics of the flow characterizes each of the four ranges depicted in figure 1. However, it must be remarked that the characterization is by no means exact for the following reasons. First, the Reynolds number at which laminar bubbles vanish for a smooth cylinder is not equal to the critical Reynolds number, but somewhere in the stage of increasing C_d (Achenbach 1971). Secondly, there is no clear indication as to the presence of laminar bubbles for very rough cylinders where C_d has still a critical minimum, as will be shown later. Since the main purpose of the present paper is to discuss the effect of roughness on the C_d versus R relation, the present paper adopts the terminology based directly on the C_d versus R curve rather than that based on the physics of the flow.

As is well known, experimental data for a two-dimensional circular cylinder from various sources have been scattered owing to the difference in experimental conditions. These include the cylinder length-to-diameter ratio, the tunnel blockage ratio, the model end conditions, the free-stream turbulence characteristics, and, in the case of a smooth cylinder, the degree of surface smoothness. As a result it is difficult to make an exact comparison of the existing data. In the present paper measurements by Roshko (1961), Jones *et al.* (1969) and Achenbach (1971) are chosen for comparison. For references to a more extensive collection of other works, see Güven *et al.* (1980).

5. The experimental results and discussions

5.1. *Smooth cylinder and cylinders with distributed roughness*

Figure 2 shows the variations of the drag coefficients with Reynolds number for a smooth cylinder and cylinders with distributed roughness, together with that for a smooth cylinder with 3·2 mm diameter roughness strips at $\theta = 50°$. Measurements by Roshko (1961) and Jones *et al.* (1969) on smooth cylinders and those by Achenbach (1971) on a cylinder with distributed roughness are also included for comparison. Figures 3 and 4 show respectively the corresponding variations of the base pressure coefficient and the Strouhal number with Reynolds number. In these figures data for the subcritical range are omitted because signals from the pressure transducer were then poor owing to low dynamic pressures, particularly for the smooth cylinder. A selection of the measured pressure distributions is given in figures 5 and 6; in most cases, except near the critical Reynolds number, there was no significant difference in pressure coefficient between the upper and the lower side, so that values averaged on the two sides are plotted in the figures.

In figure 2 the drag coefficient for the smooth cylinder falls abruptly to a minimum value of about 0·25 at $R \approx 5{\cdot}0 \times 10^5$, and then increases slightly with R. It appears that the drag coefficient approaches the curve of Jones *et al.* (1969) rather than that of Roshko (1961) at higher Reynolds numbers (transcritical range); Roshko (1970) suspects that there might have been some effect of surface roughness in his smooth-cylinder measurements.

The variation of C_d for the cylinder with distributed roughness of $r/D = 1000 \times 10^{-5}$ is in good agreement with that of Achenbach (1971), which had nearly the same roughness parameter of 818×10^{-5} ($k_s/D = 450 \times 10^{-5}$ in Achenbach's notation). Figure 2 indicates that the main effect of roughness is to cause earlier transition to the critical, thereby accompanying an increase in the minimum C_d. Also,

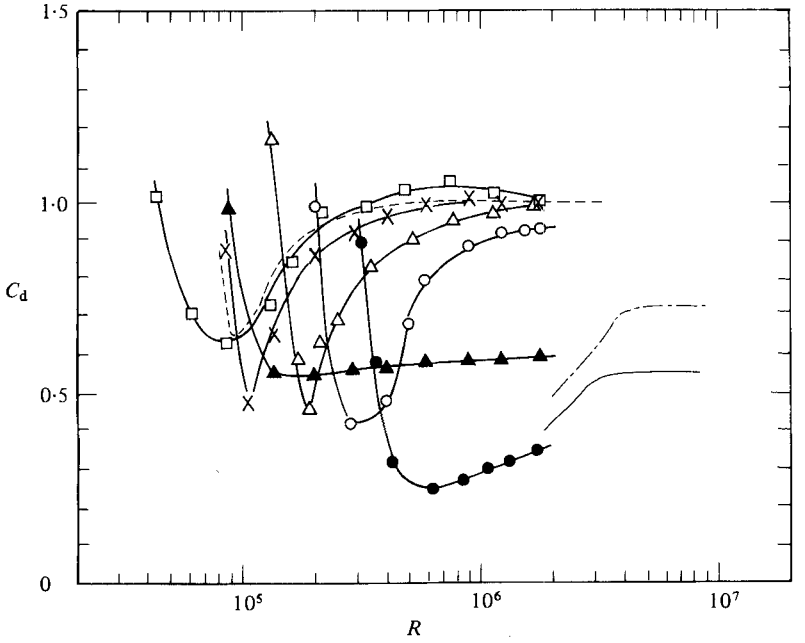

FIGURE 2. Drag coefficient. Smooth cylinders: —·—·—, Roshko (1961); ——, Jones *et al.* (1969); ●, present experiments. Cylinders with distributed roughness: – – – –, Achenbach (1971), $r/D = 881 \times 10^{-5}$ ($k_s/D = 450 \times 10^{-5}$); □, present experiments, $r/D = 1000 \times 10^{-5}$; ×, 516×10^{-5}; △, 226×10^{-5}; ○, 90×10^{-5}. Smooth cylinder with 3·2 mm diameter roughness strips at $\theta = 50°$: ▲, present experiments.

in agreement with Achenbach (1977), the drag coefficients corresponding to the three larger roughnesses approach a common level in the transcritical range. Figure 3 shows that the variations of $-C_{pb}$ with R are similar to the corresponding variations of C_d with R. Figures 5 and 6 show that the decrease of C_{pb} due to roughness is closely related to the decrease of the pressure recovery $C_{pb}-C_{pm}$, although roughness also increases the minimum pressure C_{pm}. Güven *et al.* (1980) suggested that larger roughness gives rise to a thicker and more retarded boundary layer, which separates earlier and with a small pressure recovery.

In agreement with Szechenyi (1975), very regular vortex shedding was present for cylinders with distributed roughness in the super-and transcritical ranges as well as in the subcritical range. At Reynolds numbers close to the critical, the flow was often unstable, so that the spectra of the hot-wire signals became broad-banded. As shown in figure 4, S decreased to about 0·21–0·22 after jumping to high values at around the critical Reynolds numbers.

Incidentally, as the inset in figure 5 indicates, the base pressure in the transcritical range was found to be very uniform along the span. In other words, the flow in the transcritical range could maintain good two-dimensionality. In contrast, the flow near the critical Reynolds number often yielded unsymmetrical pressure distributions, as exemplified in figure 6 for the case of the cylinder with distributed roughness of $r/D = 90 \times 10^{-5}$ at $R = 4{\cdot}0 \times 10^5$. Another point that is worth mentioning is that the pressure on the cylinder with distributed roughness of $r/D = 1000 \times 10^{-5}$ slightly decreases downstream of the separation point. The decrease in pressure could probably be related to regular vortex shedding, since the rear stagnation point is

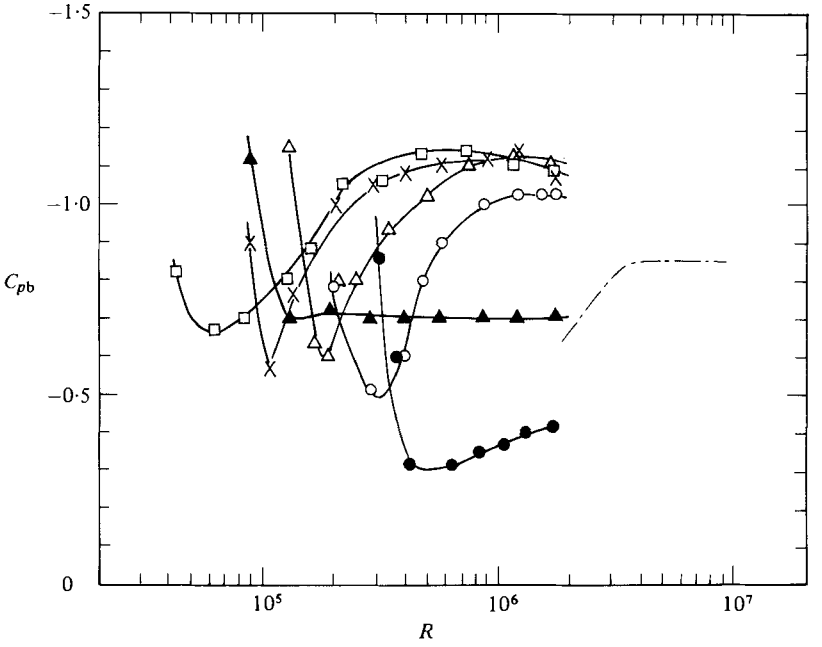

FIGURE 3. Base pressure coefficient. Notation is as in figure 2.

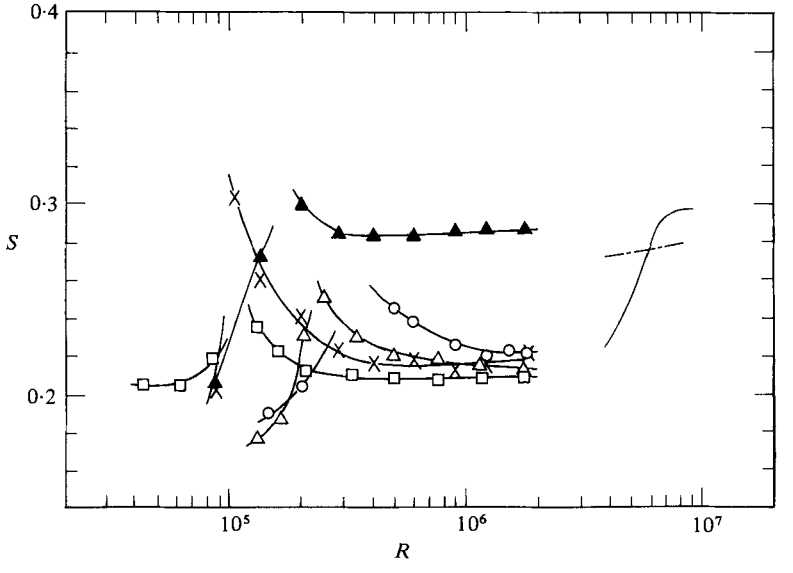

FIGURE 4. Strouhal number. Notation is as in figure 2.

closest to the downstream low pressure region where periodic vortices are formed. It was also observed in a more distinct form for a D-section cylinder (Nakamura & Tomonari 1981).

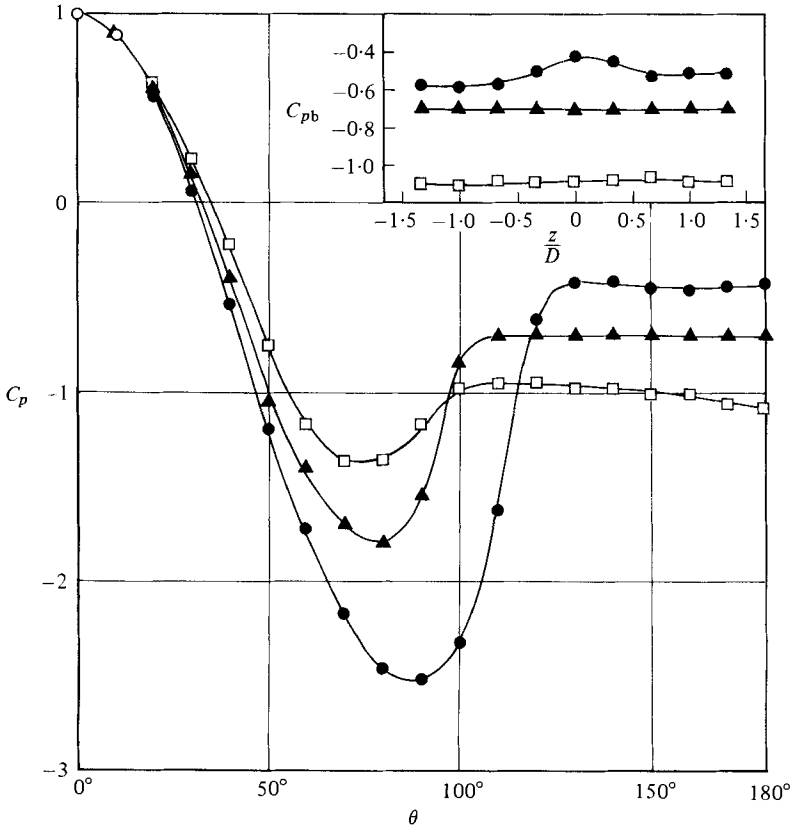

FIGURE 5. Pressure distributions at $R = 1{\cdot}7 \times 10^6$. ●, smooth cylinder; ▲, smooth cylinder with 3·2 mm diameter roughness strips at $\theta = 50°$; □, cylinder with distributed roughness, $r/D = 1000 \times 10^{-5}$.

5.2. *Smooth cylinder with roughness strips*

The experiments on a smooth cylinder with roughness strips were aimed at a simulation for the transcritical flow past a smooth cylinder by means of artificial transition of the boundary layer due to roughness. In figure 2 the drag coefficient for a smooth cylinder with 3·2 mm diameter roughness strips at $\theta = 50°$ decreases abruptly at $R = 1{\cdot}3 \times 10^5$, which is fairly low compared with $R = 5{\cdot}0 \times 10^5$ corresponding to the smooth cylinder, and furthermore it remains surprisingly constant and falls in between those of Roshko (1961) and Jones *et al.* (1969) in the transcritical range. The pressure distribution, an example of which is given in figure 5, was also found to remain unchanged over this range of Reynolds number. In the pressure measurements, it was necessary to remove any roughness elements if they were immediately upstream of the pressure taps at $\theta = 50°$; this is because the pressures at $\theta = 50°$ then indicated very low values. As shown in figure 4, very regular vortex shedding was also observed on the smooth cylinder with roughness strips. The Strouhal number remained constant over the Reynolds-number range $3{\cdot}0 \times 10^5 - 1{\cdot}7 \times 10^6$, and equal to about 0·28, which fell in between those of Roshko (1961) and Jones *et al.* (1969).

In order to look into the boundary-layer characteristics on the smooth cylinder with roughness strips, three hot wires were placed 1 mm away from the cylinder

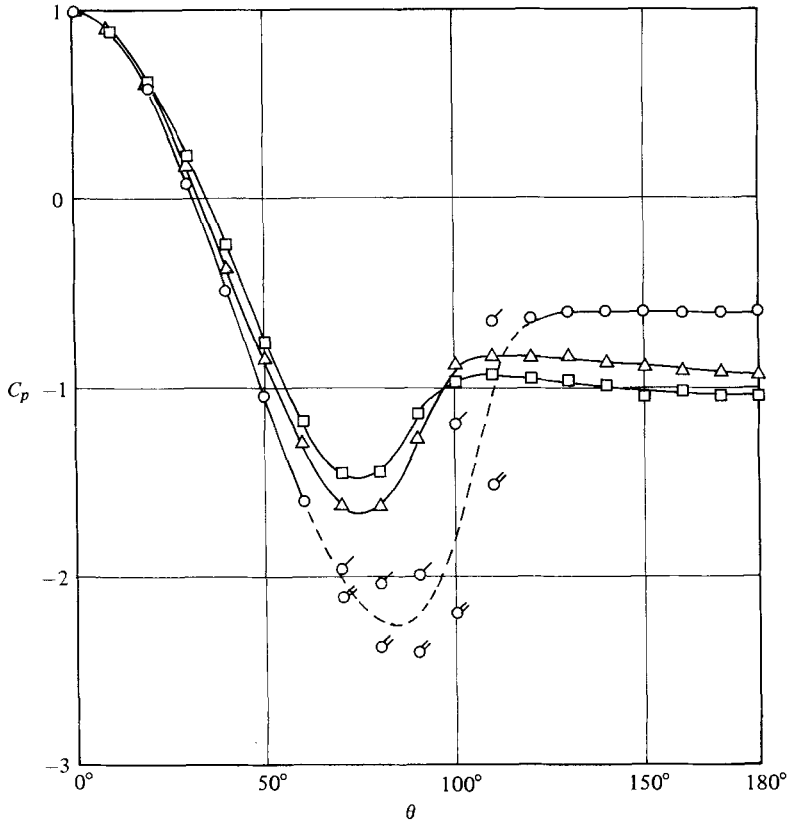

FIGURE 6. Pressure distributions on cylinders with distributed roughness at approximately the same Reynolds number. □, $r/D = 1000 \times 10^{-5}$, $R = 3{\cdot}2 \times 10^5$; △, 226×10^{-5}, $3{\cdot}4 \times 10^5$; ○, 90×10^{-5}, $4{\cdot}0 \times 10^5$, ♂, upper side, ♂, lower side.

surface: one immediately upstream of the roughness strip, one immediately downstream and another at $\theta = 60°$. At $R = 1{\cdot}5 \times 10^5$, close to the critical Reynolds number, the signal of the hot wire immediately downstream of the roughness strips indicated strong periodicity of about 800 Hz, possibly caused by the Tollmien–Schlichting-type instability. At $R = 2{\cdot}0 \times 10^5$ the high-frequency periodicity was replaced by randomness superimposed on regular vortex shedding with a much lower frequency of about 2·4 Hz, which indicated that the boundary layer just downstream of the roughness strip became fully turbulent.

It is interesting to see how particle size and strip location affect the flow characteristics. Figure 7 shows the variations with R of the uncorrected base pressure coefficients corresponding to four combinations of particle size and location. It appears from figure 7 that the 3·2 mm diameter roughness strips at $\theta = 50°$ would be an optimum selection for a simulation purpose. This is in agreement with the measurements by Maxworthy (1969) and Groehn (1974), which also found $\theta \approx 50°$ to be effective for tripping wires.

5.3. *Rough cylinders with roughness strips*

In order to get further insight into the effect of roughness on the flow past a circular cylinder, several additional experiments were made. In figure 8, a comparison is made

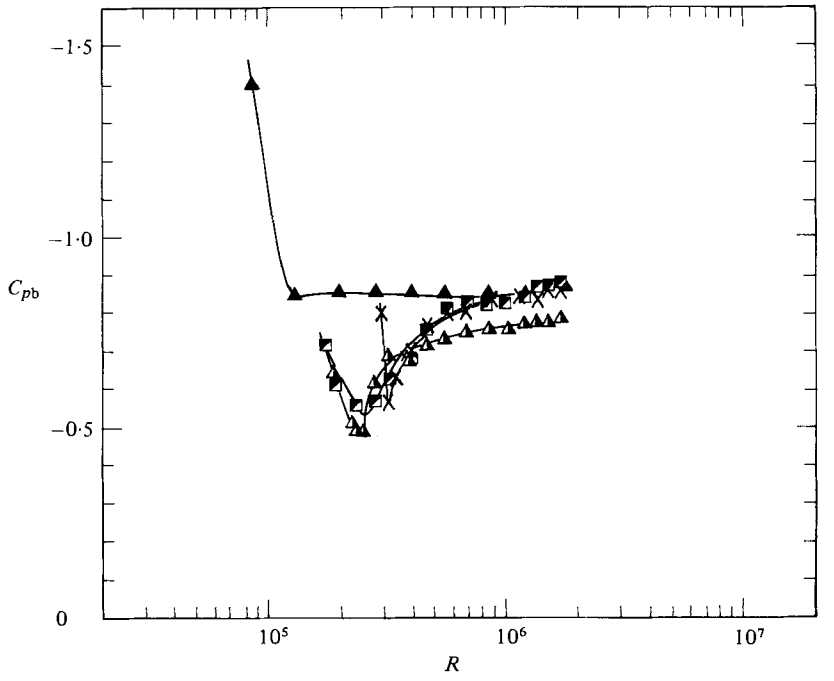

FIGURE 7. Uncorrected base pressure coefficients for smooth cylinders with roughness strips. ▲, 3·2 mm diameter roughness strips at $\theta = 50°$; ◩, 3·2 mm diameter roughness strips at $\theta = 30°$; ×, 0·56 mm diameter roughness strips at $\theta = 50°$; ⧋, 0·56 mm diameter roughness strips at $\theta = 70°$.

of the uncorrected pressure distributions on two models; one is a cylinder with distributed roughness in a restricted range $\theta = 50°$–$130°$, and the other is a cylinder with distributed roughness over the whole surface, both having the same roughness parameter $r/D = 516 \times 10^{-5}$ and $R = 1{\cdot}8 \times 10^6$. It is interesting that in agreement with a previous measurement (Okajima & Nakamura 1973; see also Nakamura 1975) the two pressure distributions are almost identical, except for a very high value of C_p at $\theta = 50°$ of the former cylinder, which was due to a local flow separation caused by the roughness discontinuity. The experiments indicated that good agreement was obtained for all the Reynolds numbers greater than about $R = 1{\cdot}3 \times 10^5$. Judging from Achenbach (1971), the upstream movement of the transition point over the same Reynolds-number range would be considerable, and could possibly be from about $\theta = 50°$ to 20°. Therefore it is suggested that only the roughness in the turbulent boundary layer between $\theta = 50°$ and the separation point can play a vital role in determining the overall flow characteristics.

Figures 9 and 10 show respectively the base pressure coefficient and the Strouhal number, both uncorrected, for cylinders with 3·2 mm diameter roughness strips at $\theta = 50°$ in which roughness on the part of the surface downstream of the roughness strips was provided either with polystyrene particles or with the sandpaper. The corresponding results for the smooth cylinder with roughness strips are also given for comparison in both figures. The general trend indicated in figure 9 is clear. That is, as the critical Reynolds number is exceeded, the value of $-C_{pb}$ remains constant and equal to that for the smooth cylinder with roughness strips, and then increases straightforwardly to a plateau at high Reynolds numbers. In short, the effect of roughness on the development of the turbulent boundary layer, or at least on its

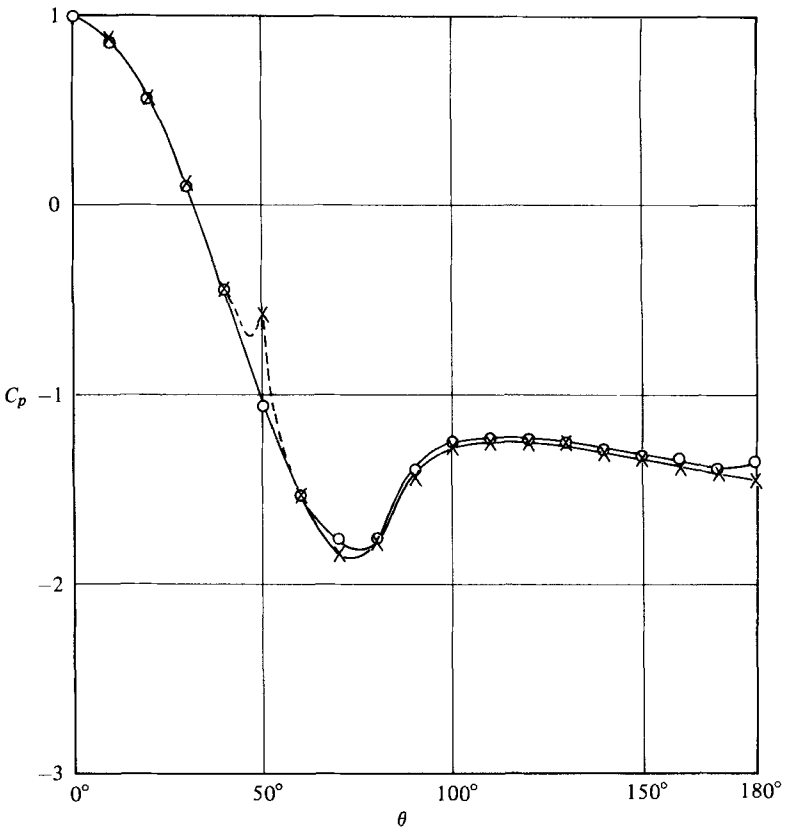

FIGURE 8. Uncorrected pressure distributions on cylinders with distributed roughness. $r/D = 516 \times 10^{-5}$, $R = 1{\cdot}8 \times 10^6$. ○, roughness distributed over the whole surface; ×, roughness distributed over $\theta = 50°$–$130°$.

separation from the cylinder surface, is negligible initially and then manifests itself. Increasing roughness lowers the Reynolds number at which $-C_{pb}$ begins to increase, and raises the level of the plateau at higher Reynolds numbers. The variations of the Strouhal number shown in figure 10 are in good correspondence with those of the base pressure coefficient shown in figure 9.

5.4. *Validity of high-Reynolds-number simulation*

As to the validity of the high-Reynolds-number simulation using the smooth cylinder with roughness strips at $\theta = 50°$, the following may be inferred from the discussions relating mainly to figure 9. First, the boundary layers downstream of the roughness strips became turbulent at a Reynolds number as low as about $3{\cdot}0 \times 10^5$. Secondly, the cylinder surface was found to be hydraulically smooth. Thirdly, the measured C_d, $-C_{pb}$ and S were all independent of R. It follows that the important transcritical-flow characteristics of a hydraulically smooth circular cylinder have been realized in this simulation.

Presumably the turbulent boundary layer on the simulated cylinder would be much thicker than that on the natural one. It remains therefore to know how large this effect would be. As shown in figures 2 and 4, C_d and S for the simulated cylinder fall in between those of Roshko (1961) and Jones *et al.* (1969). Assuming that

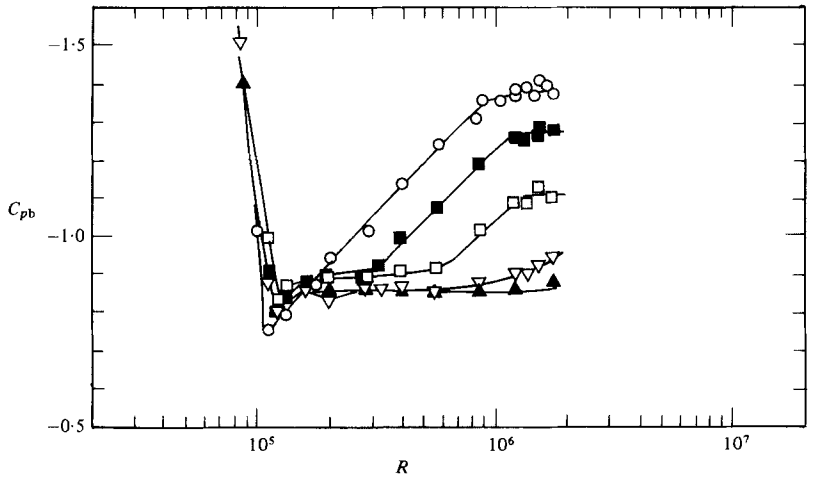

FIGURE 9. Uncorrected base pressure coefficients for cylinders with 3·2 mm diameter roughness strips at $\theta = 50°$ and with distributed roughness downstream. ▲, smooth; ○, roughness particles, $r/D = 90 \times 10^{-5}$; ■, sandpaper, C-100, $r/D = 18{\cdot}5 \times 10^{-5}$; □, sandpaper, C-180, $r/D = 9{\cdot}4 \times 10^{-5}$; ▽, sandpaper, C-400, $r/D = 6{\cdot}5 \times 10^{-5}$.

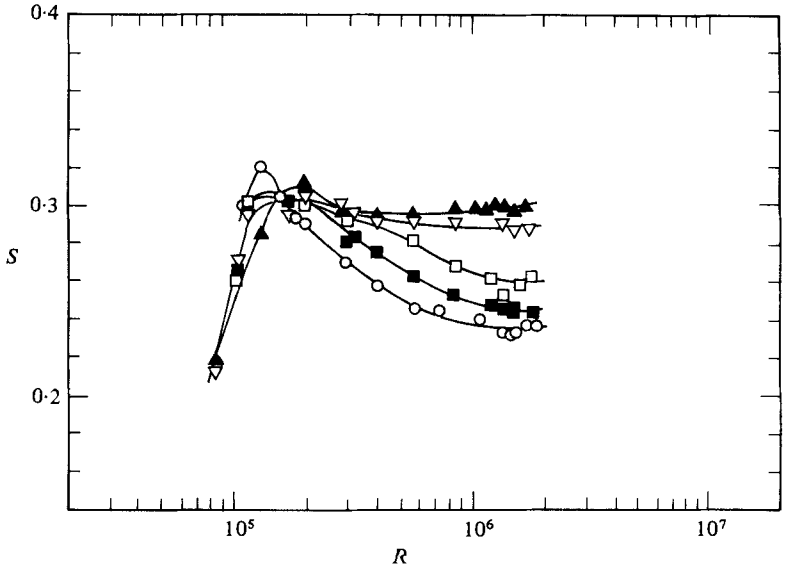

FIGURE 10. Uncorrected Strouhal numbers for cylinders with 3·2 mm diameter roughness strips at $\theta = 50°$ and with distributed roughness downstream. Notation is as in figure 10.

the correct values would be somewhere between these two measurements, it can be said that the effect of the boundary-layer thickness in the simulation was negligibly small.

Finally, it should be added that the applicability of simulation might be restricted to some of the integrated flow parameters such as the pressure distribution and the Strouhal number, since the local skin-friction coefficient and therefore the local heat-transfer coefficient, for example, might differ for the simulated cylinder and the natural one (Achenbach 1977).

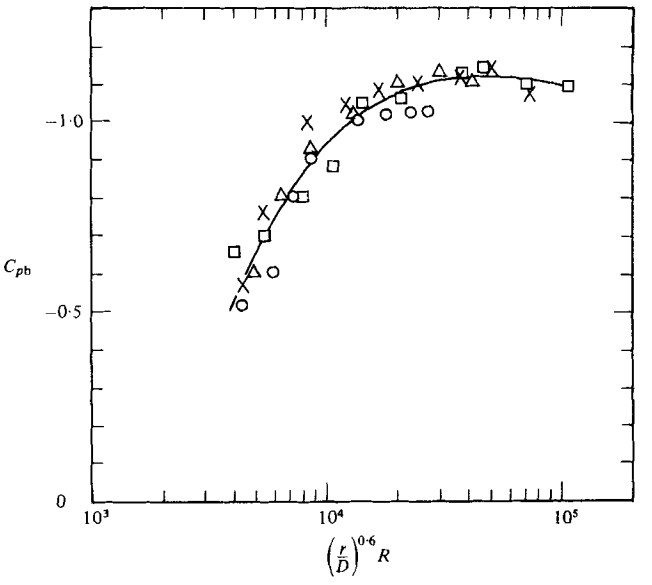

FIGURE 11. Base pressure coefficients for cylinders with distributed roughness. Notation is as in figure 2.

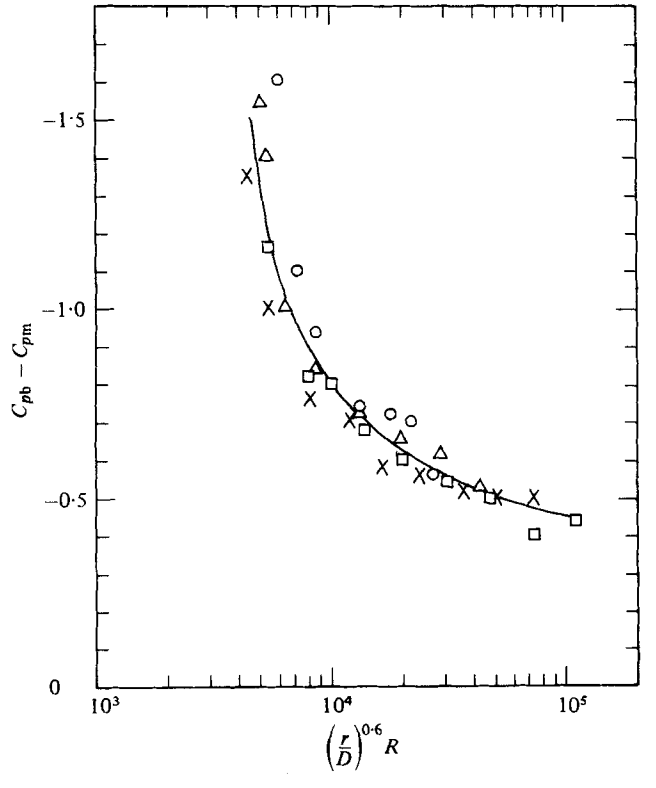

FIGURE 12. Pressure recovery $C_{pb}-C_{pm}$ for cylinders with distributed roughness. Notation is as in figure 2.

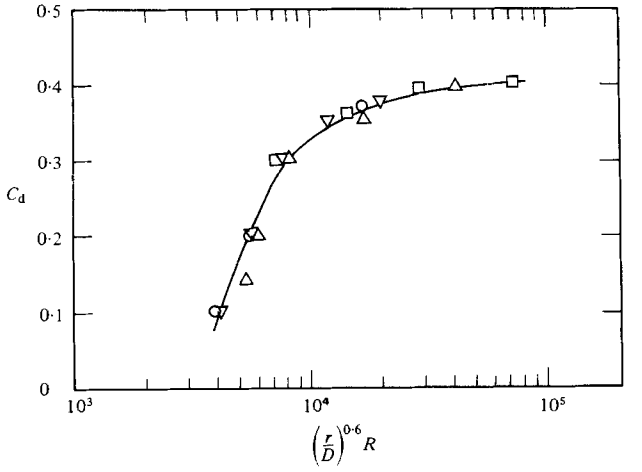

FIGURE 13. Drag coefficients of spheres with distributed roughness. Data are taken from Achenbach (1974). □, $r/D = 1250\times10^{-5}$; △, 500×10^{-5}; ▽, 250×10^{-5}; ○, 150×10^{-5}.

5.5. *A similarity parameter correlating the pressure distributions on the cylinders with distributed roughness*

The flow past a two-dimensional circular cylinder with distributed roughness is a function of Reynolds number R and roughness parameter r/D, apart from the turbulence characteristics of the approaching flow. Szechenyi (1975) claimed that a single parameter, called the roughness Reynolds number, which is defined as the product of R and r/D, could correlate the drag coefficient C_d and r.m.s. lift coefficient C_{Lrms} due to vortex shedding for cylinders with distributed roughness in the super- and transcritical ranges. Güven *et al.* (1980), however, cast doubt about the validity of Szechenyi's roughness Reynolds number.

Figure 9 suggests that although the level of the plateau of $-C_{pb}$ in the transcritical range is dependent on the roughness parameter r/D, contrary to Szechenyi's expectation, there might be some similarity parameter applying to the range where $-C_{pb}$ is increasing; that is, the supercritical range. This possibility has been explored by looking for a similarity parameter of the form $(r/D)^m R$ in the present measurements. It has been found that a similarity parameter with an exponent $m = 0{\cdot}6$ can correlate the pressure distributions on all four cylinders with different distributed roughnesses obtained in the present measurements.

Figure 11 shows the correlation of $-C_{pb}$ with $(r/D)^{0{\cdot}6}R$, while figure 12 shows that of the pressure recovery $C_{pb}-C_{pm}$. It is seen from these figures that the degree of correlation is satisfactory, although there remain some small scatters in both figures. It is also very interesting to note that even better correlation has been found using the same similarity parameter for the drag coefficients of spheres with distributed roughness which Achenbach (1974) obtained in his measurements. This is shown in figure 13.

Finally, a comment should be made concerning the physical basis for the present similarity parameter. What is clear is that the pressure distribution, while it is originally a function of two parameters r/D and R, is reduced to be a function of a single parameter. As in the classical work of Nikuradse (1933) on the flow past rough pipes, the most important physical parameter relevant to the present problem would

be the height of roughness relative to the thickness of the viscous sublayer of the turbulent boundary layer. Possibly, the similarity parameter mentioned could be related to this ratio. Further study needs to be made to elucidate the point.

6. Conclusions

The measurements of the mean-pressure distribution and the Strouhal number on a smooth circular cylinder, circular cylinders with distributed roughness and circular cylinders with roughness strips were made over a Reynolds-number range $4{\cdot}0 \times 10^4$–$1{\cdot}7 \times 10^6$ in a uniform flow. The main conclusions are summarized below.

The results on circular cylinders with distributed roughness are in good agreement with Achenbach (1971). A successful high-Reynolds-number (transcritical) simulation for a smooth circular cylinder is made using a smooth circular cylinder with roughness strips at $\theta = 50°$ at low Reynolds numbers, greater than about $3{\cdot}0 \times 10^5$. High-Reynolds-number simulation can only be obtained by roughness strips, and not by distributed roughness. If there is roughness downstream of the roughness strips then the turbulent boundary layers are retarded and separate earlier owing to roughness, resulting in a larger drag coefficient. In the transcritical range the overall flow characteristics are primarily functions of the roughness parameter r/D. A similarity parameter $(r/D)^{0{\cdot}6}R$ can correlate the pressure distributions on circular cylinders with distributed roughness in the supercritical range where the drag coefficient is increasing with Reynolds number. The same parameters also correlates the drag coefficients of spheres with distributed roughness.

We are most grateful to Professor I. Tani for encouragement and useful suggestions. Dr C. Farell, University of Minnesota, has provided helpful comments on the earlier version of the manuscript. Technical assistance from Mr K. Watanabe and Mr S. Kashiwada in conducting the experiment is gratefully acknowledged. This work was supported in part by a grant from the Ministry of Education, Science and Culture, Japan.

REFERENCES

ACHENBACH, E. 1968 *J. Fluid Mech.* **34**, 625.

ACHENBACH, E. 1971 *J. Fluid Mech.* **46**, 321.

ACHENBACH, E. 1974 *J. Fluid Mech.* **65**, 113.

ACHENBACH, E. 1977 *Int. J. Heat Mass Transfer* **20**, 359.

ALLEN, H. J. & VINCENTI, W. G. 1944 *NACA Tech. Rep.* no. 782.

FAGE, A. & WARSAP, J. H. 1929 *Aero Res. Comm.* no. 1283.

FARELL, C. 1981 *Proc. A.S.C.E.: J. Engng Mech.* **107** (EM3), 565.

GROEHN, H. G. 1974 Über den Einfluß von Stolperdrähten auf die Umströmung eines Kreiszylinders. Ph.D. dissertation, Technical University Berlin.

GÜVEN, O., FARELL, C. & PATEL, V. C. 1980 *J. Fluid Mech.* **98**, 673.

GÜVEN, O., PATEL, V. C. & FARELL, C. 1977 *Trans. A.S.M.E.* I: *J. Fluids Engng* **99**, 470.

JONES, G. W., CINCOTTA, J. J. & WALKER, R. W. 1969 *NASA Tech. Rep.* R-300.

MAXWORTHY, T. 1969 *Trans. A.S.M.E.* E: *J. Appl. Mech.* **36**, 598.

NAKAMURA, Y. 1975 In *Proc. 4th Int. Conf. Wind Effects on Buildings and Structures, Heathrow* (ed. K. J. Eaton), p. 359. Cambridge University Press.

NAKAMURA, Y. & TOMONARI, Y. 1981 *Aero Q.* **32**, 153.

NIKURADSE, J. 1933 *Forsch. Arb. Ing.-Wes.* no. 361.

OKAJIMA, A. & NAKAMURA, Y. 1973 *Bull. Res. Inst. Appl. Mech., Kyushu Univ.* **40**, 387 (in Japanese).

ROSHKO, A. 1961 *J. Fluid Mech.* **10**, 345.

ROSHKO, A. 1970 In *Proc. U.S.–Japan Research Seminar on Wind Loads on Structures, Honolulu* (ed. A. N. Chiu), p. 87. University of Hawaii.

SZECHENYI, E. 1975 *J. Fluid Mech.* **70**, 529.

TANI, I. 1964 In *Preprints of IUTAM Symp. on Concentrated Vortex Motions in Fluids (org. D. Küchemann) held at the University of Michigan, Ann Arbor, Michigan*, 6–11 *July*.

TANI, I. 1967 *J. Japan Soc. Aero. Sci.* **15**, 426 (in Japanese).